Analysis of Local Heat Exchange in Combustion Chamber and Injection Nozzle of Dual-Fuel Engine

Revaz Zurabovich Kavtaradze, Dmitry Olegovich Onishchenko, Andrey Victorovich Kozlov, Alexey Stanislavovich Terenchenko, Andrey Sergeevich Golosov

Abstract: ***This work discusses features of local heat exchange in an advanced gas engine with ignition by pilot diesel fuel. Numerical study is performed using 3D nonstationary equations of energy, motion, diffusion, and continuity in the Reynolds form supplemented by k-ζ-f model of turbulence. Simultaneous combustion of gas and diesel fuels is described using the coherent flame model (CFM) supplemented by the model of ignition by pilot diesel fuel. Predictions were performed using AVL FIRE simulation package. As a consequence, the boundary conditions of the second order (local thermal flows) were determined, as well as of the third order (coefficients of heat exchange and gas temperature) with consideration for actual geometry of combustion chamber, gas exchange, and fuel injection. Local thermal loads on injection nozzle have been determined, its thermal stress–strain state has been simulated.***

Index Terms: ***dual-fuel engine, local heat exchange, mathematical simulation, natural gas, reciprocating engine.***

I. INTRODUCTION

One of the most popular methods to arrange operating process on the basis of natural gas as engine fuel is conversion of serial one-fuel engines operating on conventional diesel fuel into dual-fuel engines [1]-[3]. This work analyzes the concept of dual-fuel engine with combined mixture formation, high compression rate (characteristic for diesel engines) and ignition from pilot diesel fuel. It should be mentioned that the combined mixture formation takes place in two stages: at first external mixture formation (in inlet system prior to intake to cylinder air gas combustible mixture is formed), and then internal mixture formation (heterogeneous mixture of pilot diesel engine with homogeneous air-gas mixture is formed).

Such arrangement of operating process, in addition to improvement of engine environmental performances, modifies heat exchange in combustion chamber, especially at the tip of injection nozzle, caused not only by modification of combustion but also by significant decrease in duration of supply of diesel fuel (the amount of pilot diesel fuel is 2–5% of fuel supply at nominal operation mode). This leads to necessity to study thermal stress state of injection nozzle, which is the aim of this work. It is obvious that in order to achieve this aim, it is required to determine thermal boundary conditions of atomizer. This problem requires for detailed study of internal cylinder processes and heat transfer from fuel to nozzle, which implies simulation of local nonstationary variables of working medium in all cells of computation region (in combustion chamber for internal cylinder processes and internal space of injection nozzle upon fuel injection).

The subject of research is a four-stroke inline six-cylinder dual-fuel engine on the basis of KamAZ-910, with supercharge and intermediate cooling of charging air. The main specifications of the engine are as follows: D/S = 130/150 mm/mm, compression rate: ε = 17.5, power: 354 kW at 1400 RPM.

II. MATHEMATICAL MODEL OF OPERATION AND LOCAL HEAT EXCHANGE IN COMBUSTION CHAMBER OF DUAL-FUEL ENGINE

The mathematical model of nonstationary transfer based on fundamental equations of momentum (Navier–Stokes), energy (Fourier–Kirchhoff), concentration (Fick) and continuity is described in details in publications devoted to reciprocating engines [4]. The set of these equations is solved using the averaging method of variables of turbulent gas flow proposed by Favre [5], [6] where the density ρ is the weight function. As a consequence of averaging, the equations of transfer are in the Reynold form:

$$\bar{\rho}\frac{D\overline{W_i}}{Dt} = \overline{G_i} - \frac{\partial \bar{p}}{\partial x_i} + \frac{\partial}{\partial x_j}\left[\mu\left(\frac{\partial \overline{W_i}}{\partial x_j} + \frac{\partial \overline{W_j}}{\partial x_i} - \frac{2}{3}\delta_{ij}\frac{\partial \overline{W_k}}{\partial x_k}\right) - \bar{\rho}\cdot\overline{W_i'W_j'}\right];$$

$$\bar{\rho}\frac{D\bar{H}}{D\tau} = \bar{G}_i\overline{W}_i + \frac{\partial \bar{p}}{\partial t} + \frac{\partial}{\partial x_i}\left(\bar{\tau}_{ij}\overline{W}_j\right) + \frac{\partial}{\partial x_j}\left(\lambda\frac{\partial \bar{T}}{\partial x_j} - c_p\bar{\rho}\cdot\overline{T'W_j'}\right) + \bar{w}_r\bar{Q}_r + \frac{\partial \bar{q}_{R_j}}{\partial x_j}; \quad (1)$$

$$\frac{\partial \bar{\rho}}{\partial \tau} + \frac{\partial}{\partial x_j}\left(\bar{\rho}\cdot\overline{W}_j\right) = 0;$$

$$\frac{D\bar{C}}{D\tau} = \frac{\partial}{\partial x_j}\left(D\frac{\partial \bar{C}}{\partial x_j} - \overline{C'W_j'}\right) + \overline{\dot{m}},$$

Revised Manuscript Received June 15, 2019

RevazZurabovichKavtaradze,Bauman Moscow State Technical University, Moscow, Russia.

Dmitry Olegovich Onishchenko, Bauman Moscow State Technical University, Moscow, Russia.

Andrey Victorovich Kozlov, Federal State Unitary Enterprise Central Scientific Research Automo-bileand Automotive Institute "NAMI" (FSUE "NAMI"), Moscow, Russia.

AlexeyStanislavovichTerenchenko,FederalStateUnitaryEnterpriseCentralScientificResearchAutomo-bileandAutomotiveInstitute "NAMI" (FSUE "NAMI"), Moscow, Russia.

Andrey Sergeevich Golosov, Federal State Unitary Enterprise Central Scientific Research Automo-bileand Automotive Institute "NAMI" (FSUE "NAMI"), Moscow, Russia.

where D/Dτ is the substantial derivative; ρ is the density, kg/m^3; p is the pressure, Pa; G_i is the projection of density vector of volume forces, N/m^3, onto the Ox_i axis of Cartesian coordinates; C is the concentration, kg/m^3; H is the total specific energy, J/kg; μ is the dynamic viscosity, kg/(m · s); c_p is the thermal capacity at constant pressure, J/(kg · K); w_r is the chemical reaction rate per unit volume, kg/(m^3 · s); Q_r is the amount of released heat per unit weight, J/kg; λ is the thermal conductivity, W/(m · K); δ_{ij} is the Kronecker symbol; D is the coefficient of diffusion, m^2/s ; $\dot{m}$ is the intensity of weight source (rate of weight variation of chemical component in unit volume), kg/(m^3 · s), W is the velocity vector.

The set of equations (1) is closed by the *k*-ζ-*f* model of turbulence [6], where *k* is the kinetic energy of turbulence, ζ is the normalized velocity scale, and *f* is the elliptical function of relaxation from the model by Durbin [7], [8].

Simulation of processes in wall regions of combustion chamber is carried out using wall functions where the universal variables, such as dimensionless velocity u^+ and dimensionless temperate T^+ are calculated as functions of universal coordinate y^+ in the range of $y^+ \le 11{,}63$ [9]. The profiles of velocity and temperature in wall layer are calculated as functions of y^+using wall functions proposed in [5]. Herewith, the friction stress τ_w and thermal flow q_w on wall are, respectively:

$$\tau_w = \mu_w \frac{w_p}{y_p}, \quad q_w = \lambda_w \frac{(T_p - T_w)}{y_p}, \qquad (2)$$

where λ_w is the thermal conductivity of wall layer, W/(m·K), and the index p denotes the variable value for the computation node P closest to wall which is located on logarithmic layer of thermal boundary layer at the distance y_p.

The influence of chemical combustion in Eq. (1) is considered by intensity of internal heat source q_v,W/m^3, and mass flow rate $\dot{m}$, kg/(m^3·s). These variables can be calculated using the rate of chemical combustion w_r:

$$q_v = Q_r w_r; \dot{m} = -w_r, \qquad (3)$$

where Q_r is the heat amount released during the chemical reaction per unit weight, J/kg. The rate of combustion is determined using the expanded coherent flame model (ECFM) [4]. This model is based on the concept of propagation of laminar flame, according to which the averaged over flame front rate $w_l$and the front thickness $\delta_l$depend only on pressure, temperature, and composition of fresh charge. Herewith, it is considered that the reaction starts in comparatively thin layers which separate fresh noncombusted gas from combustion products.

The model is supplemented by differential equation of transfer of flame front density written with respect to Σ – the zone of flame frame per unit volume. This equation is as follows [4]:

$$\frac{\partial \Sigma}{\partial \tau} + \frac{\partial}{\partial x_j}\left(\overline{W}_j \Sigma\right) = \frac{\partial}{\partial x_j}\left(\frac{\nu_t}{Pr_{tD}} \frac{\partial \Sigma}{\partial x_j}\right) + S_\Sigma, \qquad 4)$$

where ν_t is the turbulent kinematic viscosity; Pr_{tD} is the turbulent Prandtl number (the Schmidt number); S_Σ is the source member equaling to the difference between generated distance of flame front surface as a consequence of deformation due to turbulent combustion and annihilation of flame front surface as a consequence of reagent consumption.

Then the average rate of fuel combustion is determined as follows:

$$\overline{w}_r = -\rho_{Tp} w_l \Sigma\,, \qquad (5)$$

where ρ_{Tp} is the fuel partial density; w_l is the velocity of laminar flame depending on local pressure *p*, temperature *T* of fresh gas charge, and local coefficient of air excess α_{air}.

Numerical experiments were based on AVL FIRE CFD simulation package (Austria) [4]. The FIRE core is based on numerical method of reference volumes using the improved SIMPLE algorithm. Discretization of fundamental equations of transfer (1) is performed using interpolation scheme of the second order of accuracy for achievement of optimum running time and computation accuracy [10].

Initial data at inlet duct (or ducts for four-valve heads) were as follows: flow rate of fresh charge (or gas pressure) as well as pressure at outlet and wall temperature (piston, cylinder, face plate of engine head, surfaces of inlet and outlet ducts). Initial conditions determine temperature, pressure, kinetic energy of turbulence and its scale as well as gas velocity (including variables of vortex motion) in computation space at initial time.

Simulation determines local variables of gas in computation region (internal cylinder space, inlet and outlet ducts) in the case of rapid carburation and combustion of air fuel mix. In addition, as already mentioned, local thermal flows on surface of parts are predicted which restrict computation space of combustion chamber; effective and environmental performances of engine are determined.

The mathematical model was verified on the basis of approved 0-1D models implemented in AVL Boost software [4].

III. SIMULATION OF HEAT EXCHANGE, CARBURATION, AND COMBUSTION IN CYLINDER OF DUAL-FUEL ENGINE

Gas exchange, carburation, and combustion as well as heat exchange in cylinder of dual-fuel engine were simulated [11]. The computation region was comprised of internal space of engine combustion chamber formed by piston, head, and sleeve supplemented by spaces of inlet and outlet ducts (Fig. 1).

During engine operation there occurs reciprocal motion of piston between dead centers (LDC and UDC) as well as vertical movements of intake and exhaust valves. The piston motion is determined by kinematic diagram with known geometrical parameters of cranking mechanism (crank length L, piston stroke S). The valves move according to the laws of their motion preset in table form.

Published By:
Blue Eyes Intelligence Engineering
& Sciences Publication

In the model the nozzle is presented by atomizer tip (Fig. 2a) where several regions are highlighted aiming at determination of boundary conditions of the second (thermal flows) or the third kinds (coefficients of heat transfer and gas temperature near wall surface). These regions are illustrated in Fig. 2b.

The number of elements (reference volumes (RV)) in the grid varied from 4,988,067 RV upon bypassing and piston position in TDC to 440,000 RV upon closed intake and exhaust valves.

At engine inlet, the mix of air and natural gas was supplied with the coefficient of air excess $\alpha_{air} = 1.36$. The other initial and boundary conditions (temperature and pressure of gas at intake and exhaust, temperature of sleeve, head, piston, internal surfaces of inlet and exhaust valves) were determined by 0-1D simulation.

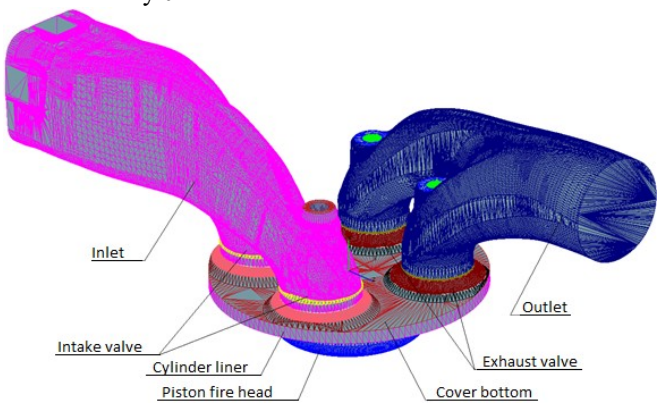

Fig. 1. Solid model of internal cylinder space, inlet and outlet ducts of the considered engine

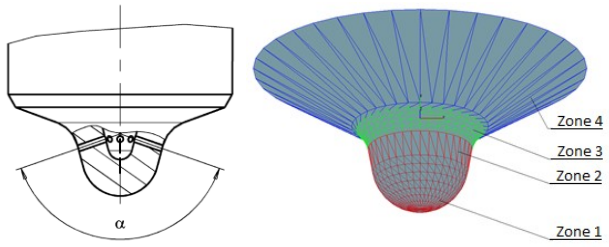

a) b)

Fig. 2. Nozzle of dual-fuel engine: a – layout of atomizing orifices, b – highlighted regions on surface of injection nozzle for subsequent determination of boundary conditions aimed at prediction of thermal stress–strain state (TSSS)

Computation started at the start of opening of inlet valve (start of bypassing, the valve gap was about 0.25 mm) at 342° CA (18° CA before TDC). Injection of pilot diesel fuel was carried out from 702 to 705° CA, the fuel amount was 0.01 g/cycle.

The model was verified by comparison of 0-1D and 3D predictions (Fig. 3). Good matching of the results can be seen both in terms of maximum pressure in cylinder and in terms of angle of its achievement: p_z differs only by 0.3 bar (248.9 bar for 0-1D and 249.2 bar for 3D predictions) at 729° CA in 0-1D and 727° CA in 3D predictions.

Upon verification of engine operation, the coherent flame model (CFM) was tuned, as a consequence the following model parameters were selected: SF = 0.16 (its decrease led to decrease in intensity of heat release) and initial density of flame front (effects on ignition delay) = 300 m^{-1}.

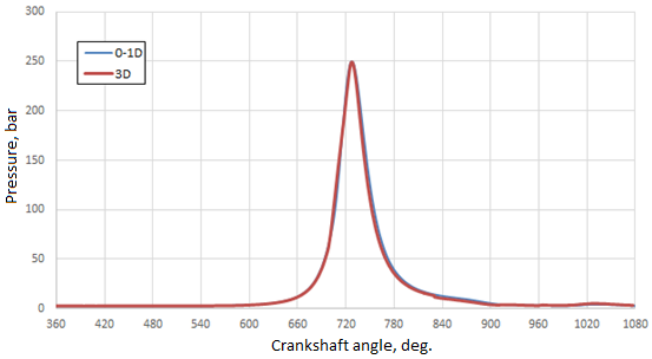

Fig. 3. Comparison of pressure diagrams obtained by 0-1D and 3D simulations (720° CA corresponds to TDC)

The pattern of heat release rate in combustion chamber of dual-fuel engine is illustrated in Fig. 4. In this case the first maximum corresponds to rapid combustion of pilot fuel and start of combustion of the main fuel, the second maximum corresponds to combustion of air gas mix in cylinder. Herewith, combustion in dual-fuel engine is characterized by uniform distribution of local variables (temperature, velocities of gas) over space of combustion chamber in comparison with diesel engine (Fig. 5), which leads to moderate rates of pressure increase in comparison with basic diesel engine at similar average effective pressure ($p_e = 25.4$ bar).

Significant value of the second maximum of heat release rate (Fig. 4) as the high maximum pressure in cylinder of the considered engine is attributed to sufficiently rich mix for diesel engine ($\alpha_{air} = 1.36$). If it is required to decrease p_z at steady charging pressure, it is possible to deplete air gas mix, to increase supply duration of pilot diesel fuel, to decrease injection advance angle.

The simulation also predicted variables of working medium in all points of the considered space for intake, cylinder scavenging, and outlet of exhaust gases.

Local variables of working medium make it possible to forecast with high accuracy the level of harmful emissions (nitrogen oxides, particulates) in engine exhaust gases. It should be mentioned that the particulates generated in cylinder of the considered dual-fuel engine due to heterogeneous combustion of pilot diesel fuel are nearly completely burnt at the time of intake opening, which improvesenvironmental performances of the dual-fuel engine.

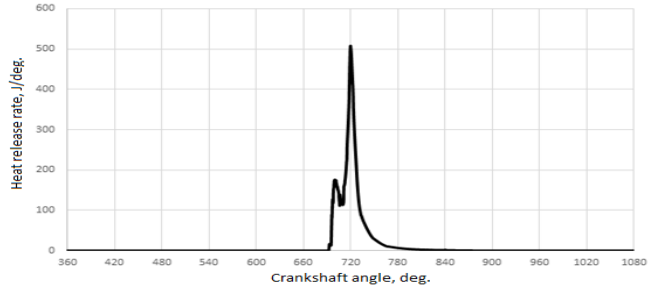

Fig. 4. Heat release rate in cylinder of the considered engine

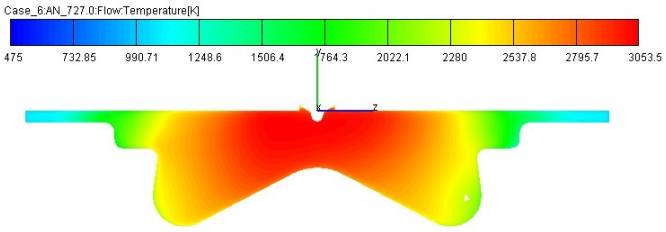

Fig. 5. Temperature distribution in cross section of combustion chamber of dual-fuel engine (φ = 727° CA, n = 1400 RPM)

In wall regions velocity and flow pattern of gas exert influence on the thickness of dynamic and thermal boundary layers and, as a consequence, on local heat exchange in these regions. In addition to the thickness of boundary layer, the intensity of heat exchange in wall region is determined by gas temperature beyond the boundary layer.

The simulation predicted heat amount released to the parts forming combustion chamber (piston, cylinder sleeve, engine cover). Averaged over cumulative surface area values of heat as a function of crank angle are illustrated in Fig. 6, and Fig. 7 shows local instant values of thermal flows in injection nozzle, determined by local temperatures and thickness of boundary layer near its surface.

An alternative representation of thermal load on injection nozzle is comprised of results presented in the form of boundary conditions of the 3rd kind (for subsequent prediction of TSSS): coefficients of heat transfer α (Fig. 8a) and local gas temperatures beyond the boundary layer (Fig. 5). Aiming at analysis, the heat amounts are shown (Fig. 8b) in the zones highlighted on the surface of injection nozzle (Fig. 2b).

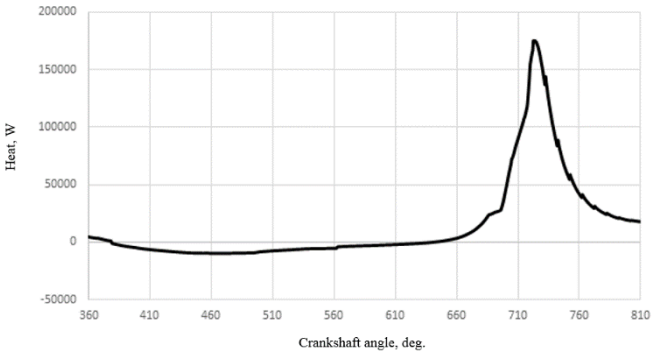

Fig. 6. Amount of heat transferred to walls of combustion chamber of dual-fuel engine

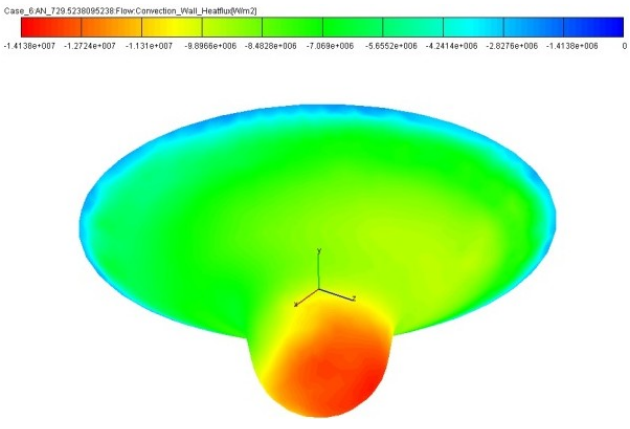

Fig. 7. Local thermal flows to injection nozzle for φ = 730°CA

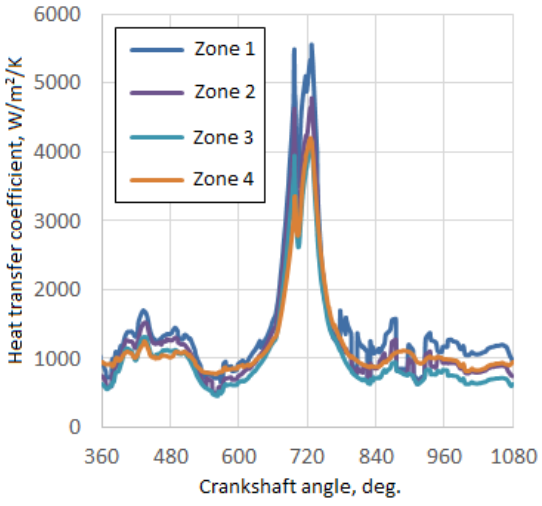

a)

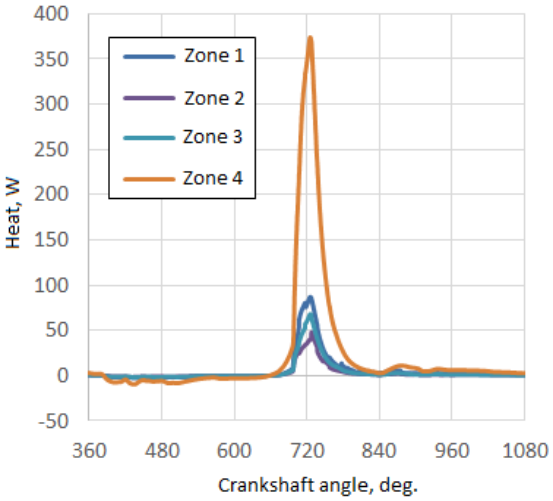

b)

Fig. 8. Distribution of coefficients of heat exchange (a) and amount of heat transferred to injection nozzle (b) averaged for zones 1–4 (see Fig. 2b) as a function of crankshaft angle of dual-fuel engine

It should be mentioned that if on the periphery of cover and piston face plate variation of this coefficient is characterized by one maximum, then in the cover center at the place of nozzle there are two such maximums (Fig. 8a). The first maximum is achieved before upper dead center, and the second maximum –after this center, herewith, the values of these maximums are close for nozzle tip (zones 1 and 2) and are significantly different for zones 3 and 4. This can be attributed to the fact that Zones 3 and 4 (rounding and atomizer periphery) are characterized by difficult access for hot gases at the first combustion stage (active combustion of pilot diesel fuel).

Then, upon development of combustion of main fuel (natural gas), hot gases penetrate into wall region, and heat transfer to atomizer surface is intensified (the second maximum in the curve α(φ), Fig. 8a). Heat transfer is also affected by variation of gas flow direction when piston passes TDC. It should be mentioned that these results agree well with previously obtained distributions of coefficients of heat transfer for engine with spark ignition and conventional fuel [11].

It is known that conversion of diesel into gas engine with spark ignition varies conditions of heat exchange, which is reflected by local thermal loads [12]-[14]. In dual-fuel engine in comparison with diesel there exists more uniform distribution of thermal flow along piston face plate after combustion start (as in engines with spark ignition). Before ignition of air fuel mixture there exists distinct heterogeneity of q_w distribution caused by gas exchange (Fig. 9a, b).

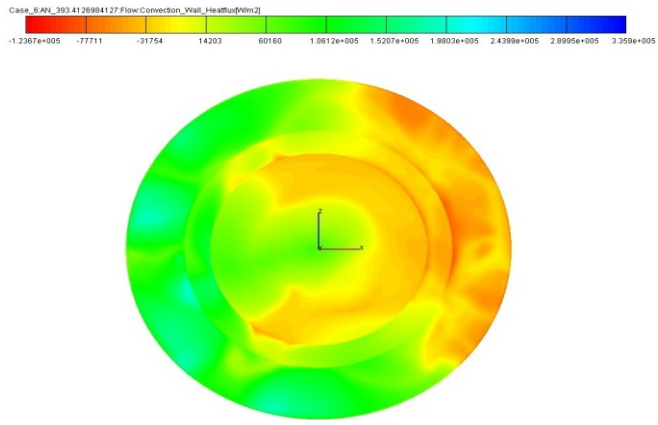

a)

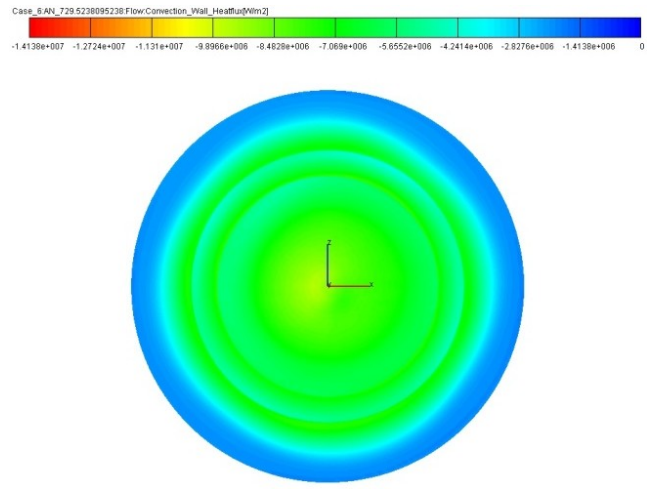

b)

Fig. 9. Thermal flows to piston face plate upon gas exchange (a, corresponds to φ = 393° CA) and combustion (b, corresponds to φ = 730° CA)

The obtained variables of heat transfer make it possible to evaluate thermal stress state of engine parts using finite element method. Thermal boundary conditions for current time (or crankshaft angle) obtained using FIRE can be applied to fixed 3D finite element partition of the parts (piston, head, cylinder liner, injection nozzle). Herewith, application of boundary conditions in computation cell (reference volume) on the part surface is not difficult since the resolution of the reference volumetric grid is usually higher than that of finite element grid, which is stipulated by specificity of the problems for gas and solid.

In steady modes, temperature varies only in thin surface layer, in the main bulk, temperature fields are considered to be stationary. In such case the boundary conditions are defined using the method proposed by Eichelberg and described in [5] according to which actual (nonstationary) thermal flows are substituted with certain resulting (equivalent) stationary flows obtained on the basis of equality of heat amount accepted by segment with the surface area of ΔF during the time (or crankshaft angle) $\Delta\varphi = \varphi_2 - \varphi_1$ in nonstationary and certain conditional stationary process.

$$\alpha_{avg} = \frac{\int_{360}^{1080} \alpha d\varphi}{720}; \quad T_{res} = \frac{\int_{360}^{1080} \alpha T_{avg} d\varphi}{720\alpha_{avg}} \qquad (6)$$

Boundary conditions of the 3rd kind (coefficients of heat transfer averaged over the area of respective surface zone of injection nozzle and crankshaft angle) and resulting gas temperatures for each zone are summarized in Table I.

Table I. Boundary conditions of the 3rd kind on the side of combustion chamber for prediction of thermal state of injection nozzle

Variable	Zone 1	Zone 2	Zone 3	Zone 4
Coefficient of heat transfer, α_{avg}, W/m^2/K	1874	1600	1409	1537
Resulting gas temperature, T_{res}, K	784	917	1042	955

It should be mentioned that significant excess of heat amount released to Zone 4 (Fig. 8b) in comparison with other zones is attributed mainly to it higher surface area. Conditions of heat exchange in this zone, as follows from Table 1, are comparable with Zone 3 (at the place of rounding, Fig. 2a), and heat exchange is characterized by lower intensity in comparison with those at the nozzle tip (Zones 1 and 2).

The obtained coefficients of heat transfer on the side of working medium in engine cylinder and gas temperature beyond boundary layer are used for determination thermal stress-strain state of injection nozzle.

IV. SIMULATION OF HEAT EXCHANGE IN INJECTION NOZZLE OF DUAL-FUEL ENGINE AND DETERMINATION OF ITS THERMAL STRESS–STRAIN STATE

Simulation of heat transfer from fuel to injection nozzle body during injection is performed in two stages: at first the variables of heat transfer upon injection are determined (in the considered gas diesel engine the duration of fuel supply φ_{inj} is 3° CA), then the obtained values are averaged for overall engine operation cycle (720° CA).

The prediction model is in this case the internal space of injection nozzle with orifices; in order to reduce computation time, one half of sector with one orifice is considered. At the orifice outlet aiming at correct simulation, cylindrical space is added (walls and cylinder surface opposite to atomizer orifice are predetermined as outlet for computations).

Boundary conditions at inlet are comprised of injection pressure (p = 1,600 bar) and fuel temperature (350 K), at outlet – pressure in cylinder of dual-fuel engine upon fuel supply (54 bar). Initial conditions for internal nozzle space are the same as for inlet: pressure (1600 bar) and fuel temperature (350 K), in cylindrical space at outlet from atomizer orifice: pressure and temperature of gas in cylinder (54 bar and 806 K). It was mentioned specially that at initial time in the injection nozzle space contained mainly (99.98%) liquid fuel, in the cylindrical space – air and vaporized fuel (also 99.98%). The remaining 0.02% in the first case are fuel and air, in the second case – fuel in liquid phase.

Symmetry conditions are preset on lateral surfaces.

Aiming at correct simulation of liquid flow in atomizer orifice, the grid upon its construction is refined (minimum cell size in this case is 0.0038 mm).

During computations the flow rate at outlet of nozzle orifice was controlled (since it was not defined as boundary condition in explicit form), its value should be 3.5 g/s for each of 8 orifices (in the mode n = 1400 RPM and supply of pilot diesel fuel equal to 10 mg/cycle, at the injection duration φ_{inj} = 3° CA).

In order to determine coefficients of heat on internal surfaces of injection nozzle, respective zones are highlighted (Fig. 10).

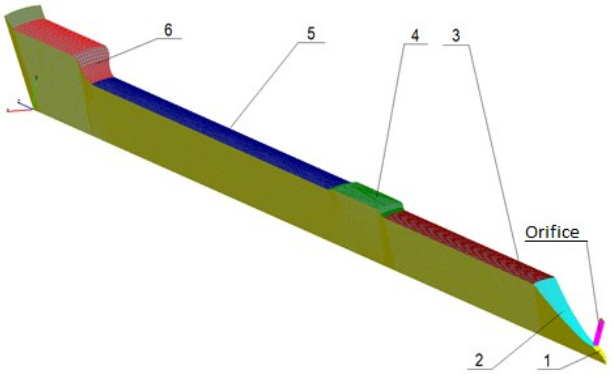

Fig. 10. Highlighted zones on internal surface of injection nozzle aiming at determination of coefficients of heat transfer

Predictions (velocity field, coefficients of heat transfer on internal surfaces) are illustrated in Figs. 11 and 12. Averaged coefficients of heat transfer and power thermal flows at the end of predictions (stationary computation) are summarized in Table 2.

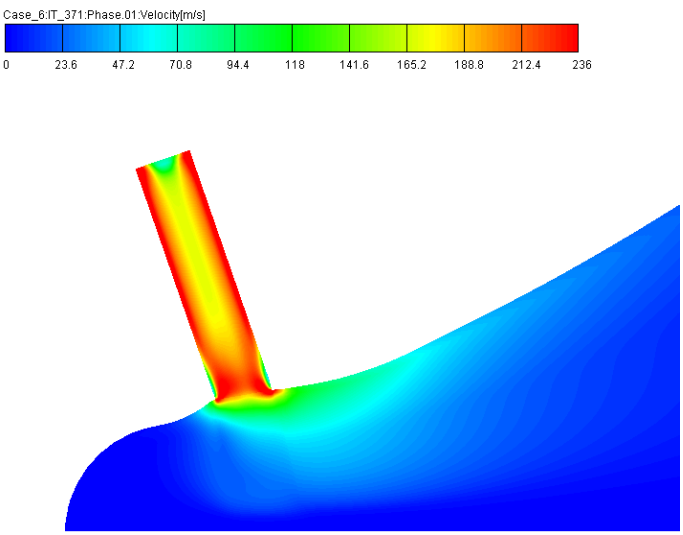

Fig. 11. Velocity field (liquid phase) in atomizing orifice upon fuel injection

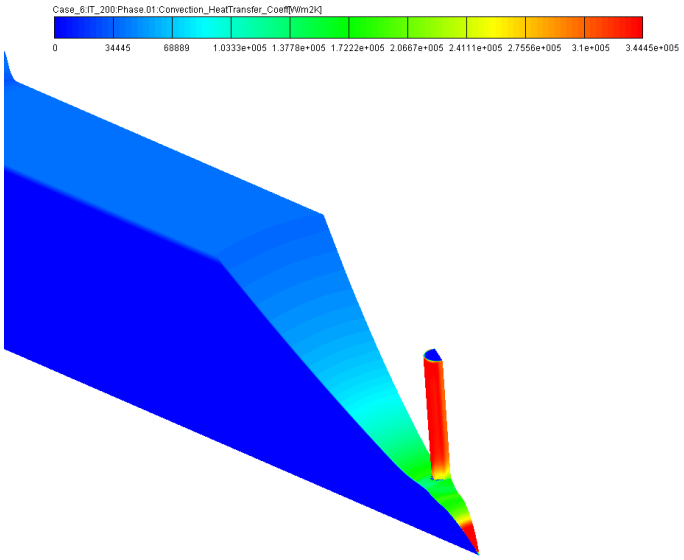

Fig. 12. Local coefficients of heat transfer in atomizing orifice upon fuel injection

Table 2. Prediction of heat transfer on the side of fuel in injection nozzle upon injection

Variable	Orifice	Zone 1	Zone 2	Zone 3	Zone 4	Zone 5	Zone 6
Coefficient of heat transfer, W/(m^2·K)	344446	257375	71032.9	39212.8	34436.3	35385.5	30507.9
Power thermal flow to wall, W	24.6	3.3	23.8	42.7	15.5	64.9	25.1

The obtained values are averaged for overall cycle of engine operation (720° CA), herewith, the coefficients of heat transfer α at the time without injections are assigned to be 1000 W/(m^2·K). Final values of α are summarized in Table 3.

Published By:
Blue Eyes Intelligence Engineering
& Sciences Publication

Table. 3. Boundary conditions of the 3rd kind on internal nozzle surfaces with consideration for duration of fuel injection (φ_{inj} = 3° CA)

Zone	Coefficient of heat transfer, W/(m^2·K)	Fuel temperature, K
Orifice	2431	350
1	2068	350
2	1292	350
3	1159	350
4	1139	350
5	1143	350
6	1123	350

The obtained boundary conditions are used for prediction of thermal stress-strain state of injection nozzle. The atomizer body is made of steel, grade KhVG, State standard GOST 5950-2000, yied point σ_y = 780 MPa.

Predictions of TSSS are comprised of two stages: at the first stage temperature field is predicted with consideration for thermal loads from hot gases in cylinder of dual-fuel engine, on the side of engine cover as well as on the side of fuel inside the nozzle. In the latter case short time supply of pilot diesel fuel is considered: in this mode the supply duration is 3° CA, at all other time fuel is motionless inside the nozzle in liquid state under high pressure (p_{int} = 1600 bar).

At the second stage mechanical loads of pressure in internal cavities of the nozzle are determined, as well as of heterogeneous heating of part (in this case the part is loaded by previously determined field as well as by internal and external pressure: p_{int} = 1600 bar, p_{ext} = 54 bar). External pressure corresponds to the conditions in combustion chamber of dual-fuel engine and is applied only to the atomizer tip.

The atomizer body during TSSS predictions is fixed to upper edges by auxiliary parts (not shown in Fig. 13).

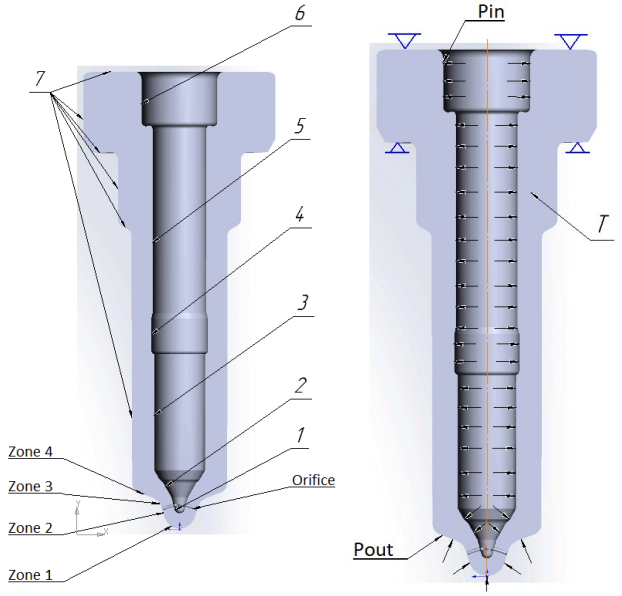

Fig. 13. Layout of fixation and loading of injection nozzle: a – thermal prediction, b – prediction of TSSS

Predictions of thermal state of injection nozzle upon its operation in combustion chamber of dual-fuel engine are illustrated in Fig. 14a. Figure 14b illustrates stresses in atomizer upon its loading with pressure on internal surfaces = 1600 bar and temperature field obtained at the first stage of predictions.

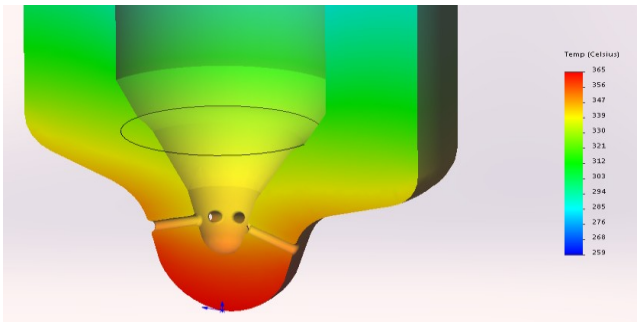

a)

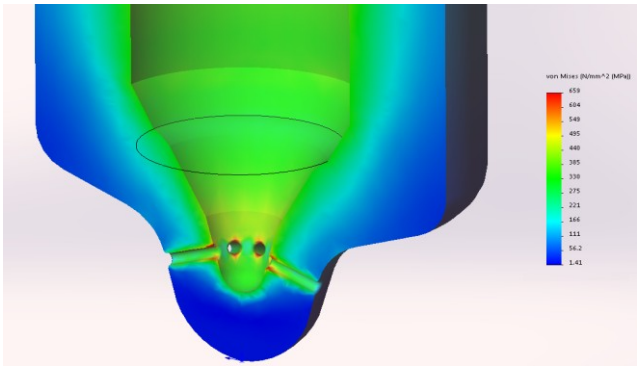

b)

Fig. 14. Predictions of temperature field (a) and stresses (b) in cross section of injection nozzle upon its operation in cylinder of dual-fuel engine

Maximum level of temperatures during nozzle operation in cylinder of dual-fuel engine is achieved at its tip equaling to 365°C (Fig. 14a). Maximum stresses upon atomizer loading with pressure corresponding to conditions of injection (1600 bar) and temperatures obtained at determination of thermal state equaled to 659 MPa (Fig. 14b), which is allowable for material of atomizer (steel, grade KhVG). The region of maximum stresses is at the place of conjunction of orifices and internal surface of atomizer.

High level of loads on injection nozzle can be observed under preset operation conditions: significant decrease in time of fuel supply to dual-fuel engine in comparison with the basic engine (3° CA and 25-30° CA, respectively) even at comparable injection pressures leads to significant increase in temperatures and stresses in atomizer tip. Nevertheless, according to predictions, the part remains in operation state.

V. CONCLUSION

The model of operation process and local heat exchange in combustion chamber was developed and verified. Its application for analysis of advanced dual-fuel engine demonstrated high accuracy of determination of local instant parameters of working medium, including velocity field, local temperatures of gas, thermal flow to parts forming combustion chamber (piston, cylinder liner, engine head, injection nozzle).

Local parameters of working medium make it possible to forecast the level of harmful emissions (nitrogen oxides, particulates) in exhaust gases. Particulates generated in cylinder of the considered dual-fuel engine due to combustion of pilot diesel fuel are nearly completely burnt at the time of intake opening, which improves environmental performances of engine.

Positive influence of gas flow pattern on heat transfer to walls of combustion chamber is mentioned. Thus, the point on engine cover (near injection nozzle) is characterized by distribution coefficient of heat transfer α with two maximum values: before and after TDC. At the same time, α has one maximum near TDC on the periphery of cover and piston face plate.

Characteristic features of heat transfer in dual-fuel engine in comparison with diesel engines include relatively uniform distribution of thermal flows along the surface of piston face plate after start of combustion (as in engines with spark ignition). Prior to air fuel mix there exists certain heterogeneity of q_w distribution caused by gas exchange.

The obtained coefficients of heat transfer on the side of working medium in engine cylinder and gas temperature beyond boundary layer make it possible to evaluate thermal state of injection nozzle. Maximum level of temperatures during nozzle operation in cylinder of dual-fuel engine is achieved at its tip equaling to 365°C. Maximum stresses upon loading pressure on atomizer corresponding to injection conditions (1600 bar) and temperatures obtained upon determination of thermal state were 659 MPa, which is allowable for material of atomizer (steel, grade KhVG).

It is mentioned that significant decrease in time of fuel supply to dual-fuel engine in comparison with basic diesel engine (3° CA and 25-30° CA, respectively) even at comparable injection pressures leads to significant increase in temperature and strains in atomizer tip. As a consequence, it is recommended to consider possibility of intensification of nozzle cooling in engine head, increase in supply duration (amount) of pilot diesel fuel, or decrease in thermal loads on the side of working medium in combustion chamber of dual-fuel engine due to lean mixture, retarded fuel injection, decrease in pressure at intake.

ACKNOLEDGMENT

Funding: The paper was prepared under the agreement No. 14.626.21.0005 with the Ministry of Education and Science of the Russian Federation (unique project identifier RFMEF I62617X0005).

REFERENCES

1. Yu.N.Vasil'ev, A.I.Gritsenko, and L.S. Zolotarevskii, “Transport na gaze” [“Transpiration on gas”]. Moscow: Nedra, 1992).
2. G.Athenstädt,“EntwiklungstationärerGasmotorenseit dem Inkrafttreten der TA- Luft”. MTZ, vol. 11. 1993.
3. R.D. Enikeev, and B.P. Rudoi, “Dvigatelivnutrennegosgoraniya. Osnovnyeterminyirussko-angliiskiesootvetstviya” [“Internal combustion engines. Main terms and Russian–English matchings”]. Moscow:Mashinostroenie, 2004.
4. FIRE. “User Manual Version 2017 / AVL List GmbH. Graz (Aus-tria), 2018.” (License Agreement for Use of the Simulation Software AVL FIRE and AVL BOOST between Moscow State Technical Univ. n.a. N.E. Bauman and AVL List GmbH, 2014).
5. R.Z. Kavtaradze, “Lokal'nyiteploobmen v porshnevykhdvigatelyakh” [“Local heat exchange in reciprocating engines”]. 3rd edition. Moscow:MGTU, 2016.
6. K.Hanjalić, M.Popovać, and M.Hadziabdić, “A Robust Near-Wall Ellip-tic-Relaxation Eddy-Viscosity Turbulence Model for CFD”.Int. J. Heat Fluid Flowvol.25,2004, pp. 897-901.
7. P.A. Durbin, “Near-Wall Turbulence Closure Modeling Without “Damping Functions””.Theoretical and Computational Fluid Dynamics, vol. 3(1), 1991, pp.1-13.
8. M.Popovać, and K.Hanjalić,“Compound Wall Treatment for RANS Computation of Complex Turbulent Flow”.Proc. 3rd M.I.T. Conference, Boston, USA, 2005,pp. 1-28.
9. H. Schlichting,“Grenzschicht-Theorie”. Karslruhe: Verlag G. Braun, 1951.
10. S. V. Patankar,“Computation of Conduction and Duct Flow Heat Transfer”. Maple Grove: Innovative Research, Inc., 1991.
11. A.A. Zelentsov, “Analizvliyaniyaosobennosteirabochikhprotsessovnaeffektivnyepokazateliaviatsionnykhporshnevykhdvigatelei” [“Influence of operating processes on effective properties of aviation reciprocating engines”].VestnikMoskovskogogosudarstvennogotekhnicheskogouniversitetaim. N.E. Baumana. Mashinostroenie,vol. 4, 2013, pp. 81-93.
12. R.Z.Kavtaradze, A.A.Zelentsov, and V.V. Krasnov, “Local Heat Transfer in Diesel Combustion Chamber Converted to Operate on Natural Gas and Hydrogen”. High Temperature, vol. 56(6), 2018, pp. 900-909.
13. N.Kh.Tuan,K.E.Karpukhin, A.S.Terenchenko, and A.F. Kolbasov,“World Trends in the Development of Vehicles with Alternative Energy Sources”. ARPN Journal of Engineering and Applied Sciences, vol. 13(7), 2018, pp. 2535-2542.
14. G.G.Ter-Mkrtichian, A.S.Terenchenko, and K.E. Karpukhin“Alternative ways for vehicle ICE development”. International Journal of Mechanical Engineering and Technology, vol. 9(5),2018, p. 966-973.

Published By:
Blue Eyes Intelligence Engineering
& Sciences Publication